Műszaki Tudományos Közlemények vol. 13. (2020) 133–136.
DOI: Hungarian: https://doi.org/10.33895/mtk-2020.13.24
English: https://doi.org/10.33894/mtk-2020.13.24

NUMERICAL MODELLING OF THE THREE-ROLL BENDING PROCESS OF A THIN PLATE

Péter MÁTÉ,[1] András SZEKRÉNYES[2]

Budapest University of Technology and Economics, Faculty of Mechanical Engineering, Department of Applied Mechanics. Budapest, Hungary

[1] *matepeter95@gmail.com*

[2] *szeki@mm.bme.hu*

Abstract

The three-roll bending process is a simple procedure, commonly used in the industry, through which a cylindrical surface can be produced from a sheet plate. This process is mainly controlled through experience and it is described with the finite element method, except for a very few numerical and analytical investigations. The topic of this article is to present a numerical method, through which the curvature function along the rolling direction can be calculated. This article presents the proposed numerical method and its verification with the finite element method. The results of the two numerical methods are in good agreement.

Keywords: *sheet metal, three-roll bending, metal forming, residual curvature.*

1. Introduction

The three-roll bending process is a simple three-point bending, with the difference that here the plate is moved through the device so that each part of it suffers bending. The device consists of two lower and one upper roller - the upper one lying between the two lower ones. First, the plate is placed between the rollers, and then it is loaded by the vertical movement of the upper roller. After this the sheet metal can be moved by rotating the lower rollers simultaneously; however, in extreme cases a proper rotation of the upper roller may be necessary. By the continuous displacement of the plate each segment will be bent along a line, and thus a cylindrical surface will be formed. The different states of the plate (at the end of the loading process, and during the moving phase) can be seen on **Figure 1**.

2. Modeling the sheet metal

To model the material's behavior, I chose an elastic- isotropic hardening plastic model, known as the von Mises bilinear model. Its stress-strain curve can be seen in **Figure 2.** This model is good for small plastic strains, or almost linear plastic characteristics. Building the calculations on it, the algorithm can be adapted later for a multilinear plastic stress-strain curve.

The relation between the stress and the strain is given by Hooke's law, and can be found in equation (1) which is adapted here for the plastic region in equation (2), by offsetting the starting point into (σ_F; ε_F). Further on, the Kirchhoff-Love theory of plates will be used. The stress and strain parameters of the constitutional equation are defined in a coordinate system connected to the plate's mid-surface. The plate will undergo pure bending, as shown in **Figure 3.**

The strain in the x direction, present in the plate, proportional to the z coordinate, is described by the equation $\varepsilon_x = \kappa \cdot z$.

$$\boldsymbol{\sigma}^e = \begin{bmatrix} \sigma_x^e \\ \sigma_y^e \end{bmatrix} = +\frac{E}{1-\nu^2} \cdot \kappa \cdot z \begin{bmatrix} 1 \\ \nu \end{bmatrix} \tag{1}$$

$$\boldsymbol{\sigma}^\mathbf{p} = \begin{bmatrix} \sigma_x^p \\ \sigma_y^p \end{bmatrix} = \begin{bmatrix} \sigma_x^F \\ \sigma_y^F \end{bmatrix} + \frac{E_T}{1-(\overline{\nu})^2} \cdot \kappa \cdot (z - z_F) \begin{bmatrix} 1 \\ \overline{\nu} \end{bmatrix} \tag{2}$$

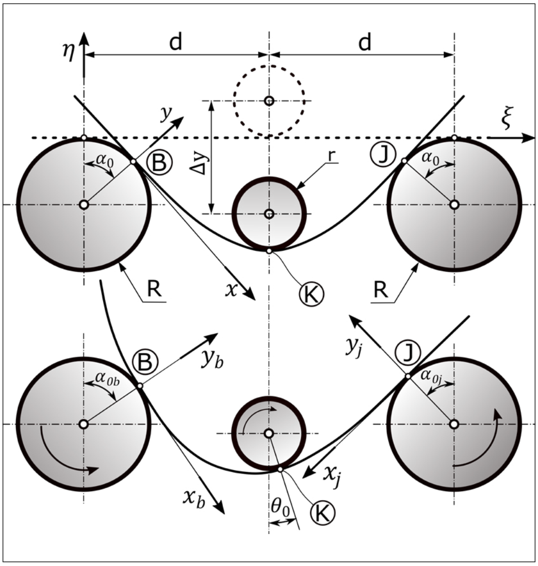

Figure 1. *The structure's sketch: first load (upper) and the displacement (lower)*

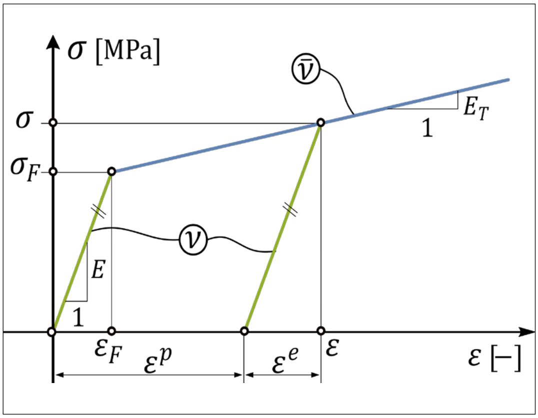

Figure 2. *The stress-strain curve of the bilinear material model.*

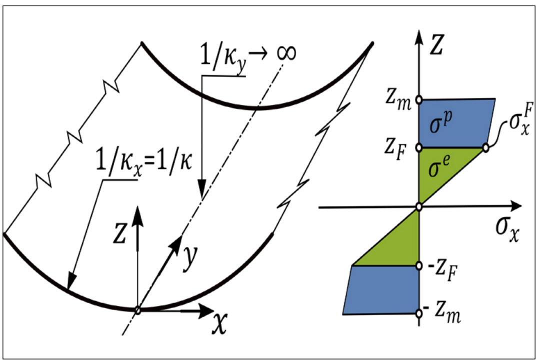

Figure 3. *Plate bending and stress distribution along the thickness.*

To obtain the parameters of the yielding point, the von Mises yield criterion will be used. The stress state on the elastic region's boundary is presented in equation (3).

$$\boldsymbol{\sigma}^{\mathbf{F}} = \begin{bmatrix} \sigma_x^F \\ \sigma_x^F \end{bmatrix} = \frac{\sigma^F}{\sqrt{1-\nu+\nu^2}} \cdot \begin{bmatrix} 1 \\ \nu \end{bmatrix} \tag{3}$$

Furthermore, it is necessary to know the boundary inside the plate between the elastic and plastic zones, and the curvature at which the yielding of the material occurs. For this the border curvature (κ_H) and the region border (z_H) along the thickness will be defined. They are presented in equations (4) and (5).

$$\kappa_H = \frac{\sigma^F}{z_m} \cdot \frac{1}{E} \cdot \frac{1-\nu^2}{\sqrt{1-\nu+\nu^2}} \tag{4}$$

$$z_F = \frac{\sigma^F}{\kappa} \cdot \frac{1}{E} \cdot \frac{1-\nu^2}{\sqrt{1-\nu+\nu^2}} \tag{5}$$

The bending moment needed for a given curvature is obtained from the integration of the stress field. The required bending moments for the elastic- (M^e) and elastic-plastic (M^p) states are given in equations (6) and (7), respectively. These moments as functions of the curvature can be seen on **Figure 4**.

$$M^e(\kappa) = \lambda \cdot \kappa \tag{6}$$

$$M^p(\kappa) = a + \frac{b}{\kappa^2} + c \cdot \kappa \tag{7}$$

The *a*, *b*, *c*, *λ* parameters are material and geometric constants, as given by equations (8)-(11)..

$$\lambda = \frac{2}{3} \cdot \frac{E}{1-\nu^2} \cdot {z_m}^3 \tag{8}$$

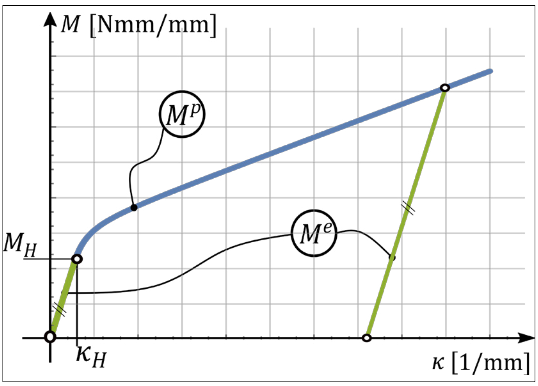

Figure 4. *The bending curve of the plate.*

$$a = \frac{{z_m}^2 \cdot \sigma^F}{\sqrt{1-\nu+\nu^2}} \cdot \left(1 - \frac{E_T \cdot (1-\nu^2)}{E \cdot (1-\bar{\nu}^2)}\right) \tag{9}$$

$$b = \frac{{\sigma_F}^3 \cdot (\nu^2-1)^2 \cdot (E + E_T \cdot (\nu^2-1) - \bar{\nu}^2 \cdot E)}{3 \cdot E^2 \cdot (1-\nu+\nu^2)^{\frac{3}{2}} \cdot (\bar{\nu}^2-1)} \tag{10}$$

$$c = \frac{2 \cdot E_T \cdot {z_m}^3}{3 \cdot (1-\bar{\nu}^2)} \tag{11}$$

2.1. The plastic Poisson's ratio

It is a commonly accepted assumption that the plastic part of the strain does not contribute to the dilatation [1]. If this assumption is applied to the bilinear model, equation (12) can be written. The function was derived for a unidirectional pull, but I assume further on, that this plastic Poisson's ratio (ν_p) will be valid for any strain state. .

$$\nu_p(\varepsilon_x) = \frac{1}{2} - \left(\frac{1}{2} - \nu\right) \cdot \left[\frac{\varepsilon_F}{\varepsilon_x} + \frac{E_T}{E} \cdot \left(1 - \frac{\varepsilon_F}{\varepsilon_x}\right)\right] \tag{12}$$

Considering that the Poisson's ratio from the constitutive equation refers only to the region after the yielding point, I define $\bar{\nu}$ with the help of equation (13).

$$\bar{\nu} = \frac{\varepsilon_y - {\varepsilon_y}^F}{\varepsilon_x - {\varepsilon_x}^F} = \frac{1}{2} - \left(\frac{1}{2} - \nu\right) \cdot \frac{E_T}{E} \tag{13}$$

3. Numerical model

3.1. Modeling tools

Due to the fact that the plate has nonzero curvature only in a single direction, its shape can be described by the projection of the mid-plane along the rollers' axes as presented in Figure 5. Here I built up the plate from finite, Δs long elements,

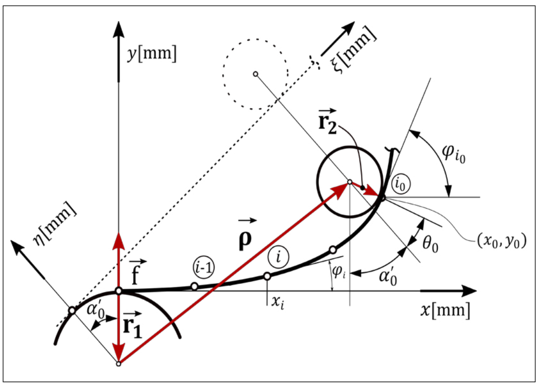

Figure 5. *Mechanical model of the plate.*

and the parameters of the nodes result from a numerical integration along the sheet. Further on, I divide the plate into a left- and a right part, and I iterate the forces acting on the sheet, until the two parts will form a C^2 class continuous curve with a proper approximation. The two parts should meet at the same ***K*** point on the central roller, and both should be at a tangent to it. The index of the node at the contact point with the central roller is always named „i_0". At the first loading, only one side of the plate should be computed because of the symmetry. This symmetry vanishes when the plate is being moved between the rollers, thus both parts should be calculated separately. The recursion for the bending moment, curvature, tangent angle and coordinates is given by equations (14)-(18).

The process is driven by the forces acting between the lower rollers and the plate, so the relation between the curvature function and the displacement of the central roller will be obtained in an indirect way. The movement of the plate is modeled by offsetting the position of the loading forces always with the same number of nodes [2]. The offset of the load and thus the contact point is fixed only for point ***B*** the other two contact points will come from the calculations.

$$M_i = \left(x_{i-1} + \Delta s \cdot cos(\varphi_{i-1})\right) \cdot |\mathbf{f}| \tag{14}$$

$$\kappa = \{\kappa^* | M_i = M(\kappa^*)\} \tag{15}$$

$$\varphi_i = \varphi_{i-1} + \Delta s \cdot \frac{\kappa_i + \kappa_{i-1}}{2} \tag{16}$$

$$x_i = x_{i-1} + \Delta s \cdot cos\left(\frac{\varphi_i + \varphi_{i-1}}{2}\right) \tag{17}$$

$$y_i = y_{i-1} + \Delta s \cdot sin\left(\frac{\varphi_i + \varphi_{i-1}}{2}\right) \tag{18}$$

In equation (15) the curvature is obtained by solving the proper equation (6) or (7), depending on which region the material is in. To get the angle of deflection in the yielded region, one must fit a second order function on the curvature for each element and obtain the change in the angle of deflection by integrating that.

3.2. Finding the contact points

At the first loading step, because of the symmetry, the angle θ_0, which can be seen on Figure 5, vanishes, and $\alpha_0 = \varphi_{i_0}$ is true. Given this, searching the contact points with the central roller turns into finding the point where equation (19) is satisfied.

$$d = (R + y_{i_0}) \cdot sin(\varphi_{i_0}) + x_{i_0} \cdot cos(\varphi_{i_0}) \qquad (19)$$

When the plate moves and the symmetry no longer exists, point ***K*** will shift on the surface of the central roller with a θ_0 angle. Vector **ρ**, seen in **Figure 5** is already considered constant; its coordinates are given in the $\xi - \eta$ frame. Here finding the a α_0' is the main task. Solving this, one calculates the sine and cosine of angle α_0' according to equation (20). The solution is there, where they satisfy the Pythagorean identity with the smallest error along the curve.

$$\begin{pmatrix} cos(\alpha_0') \\ sin(\alpha_0') \end{pmatrix} = \begin{pmatrix} \rho_\xi & -\rho_\eta \\ \rho_\eta & \rho_\xi \end{pmatrix}^{-1} \cdot \left(\begin{pmatrix} x_{i_0} \\ y_{i_0} \end{pmatrix} - \mathbf{r}_1 - \mathbf{r}_2 \right) \qquad (20)$$

4. Conclusions

The comparison of the results with a finite element method simulation can be seen in **Figure 6.** The finite element method procedure used simple, four node, quadratic plane elements in a plane stress state. Along the thickness eight elements were used, as for *A. Ktari et al.* **[3]** The curvature function of the final displaced structure at a given node is calculated as the excircle of the triangle formed of the node and its two neighbors. For this I used nodes from the mid-surface.

In **Figure 6** the curvature distribution is plotted for certain sheet metal and device parameters, without the removal of the plate, as a function of the arc length. The ***B, K, J*** points shown on the figure are marking the contact points (they can be seen in **Figure 1**) in the moment when the movement of the plate stops. Point $\boldsymbol{K^0}$ marks the contact point with the central roller after the first load step. It can be seen that this point is the peak of the curvature, which after that looks as if it would be an exponentially decreasing harmonic function.

The data used for the calculations is given in **Table 1** and **2**.

The maximal relative difference between the two functions on **Figure 6** is only 3.2 %, Thus the proposed numerical procedure is proved to be useful for further investigations.

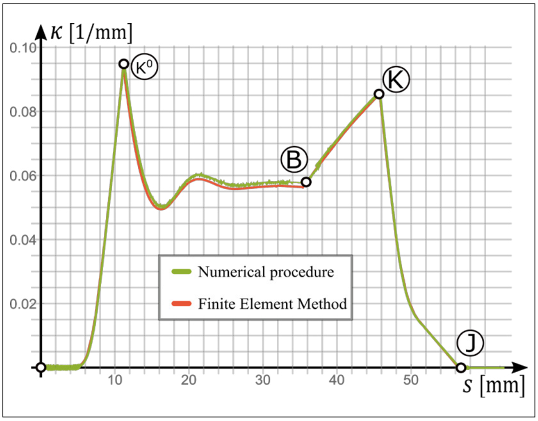

Figure 6. *Comparison of the numerical procedure with the finite element method*

Table 1. *Data for testing*

E [GPa]	E_T [GPa]	ν	σ_F [MPa]	zm [mm]
210	21	0.3	230	0.08

Table 2. *Data for testing*

R [mm]	r [mm]	Δy [mm]	d [mm]	Δs [mm]
7.5	4	4	13.5	0.001

References

[1] Shin J. G., Lee J. H., Kim Y. I., Yim H.: *Mechanics-based determination of the center roller displacement in three-roll bending for smoothly curved rectangular plates*. KSME International Journal, 15/12 (2001) 1655–1663. https://doi.org/10.1007/BF03185120

[2] NASA Technical Reports Server, *A Study of Poisson's Ratio in the Yield Region*. 1952. (letöltve: 2020. február 26.). https://ntrs.nasa.gov/archive/nasa/casi.ntrs.nasa.gov/19930083272.pdf

[3] Ktari A., Antar Z., Haddar N., Elleuch K.: *Modeling and computation of the three-roller bending process of steel sheets*. Journal of Mechanical Science and Technology, 26 (2012) 123–128. https://doi.org/10.1007/s12206-011-0936-4